



Coupling between proton binding and redox potential in electrochemically active macromolecules. The example of Polyaniline



Waldemar A. Marmisollé, M. Inés Florit, Dionisio Posadas *

Instituto de Investigaciones Físicoquímicas Teóricas y Aplicadas (INIFTA), Facultad de Ciencias Exactas, Universidad Nacional de La Plata, CCT La Plata-CONICET, Sucursal 4, Casilla de Correo 16, 1900 La Plata, Argentina

ARTICLE INFO

Article history:

Received 27 March 2013
Received in revised form 11 August 2013
Accepted 13 August 2013
Available online 27 August 2013

Keywords:

Coupling
Proton binding
Redox potential distribution
Polyaniline
Conducting polymers

ABSTRACT

In this work it is investigated the coupling between the redox potential and the extent of proton binding in electrochemically active polymers, for the particular case of Polyaniline (Pani). To this purpose, the degree of oxidation of the polymer was measured by spectrophotometry changing the external potential applied to Pani films, in solutions of different *pH* values. The knowledge of the oxidation degree for the different applied potentials allows determining the apparent formal redox potential. For Pani, in the hypothetical case of absence of interactions between the redox centres, the apparent formal redox potential should be independent of the oxidation degree and it should decrease linearly with the *pH* with a slope of 0.059 V, at room temperature. The values of the apparent formal redox potential, experimentally obtained, show that the *pH* dependence is not as expected from the redox equation. This fact implies interactions between the redox centres and some sort of coupling between the redox potential and the state of binding of the polymer. By employing a simple statistical mechanic model is possible to evaluate the interaction energy between the redox centres and also the acid dissociation constants of both, the oxidized and reduced forms. The values obtained for both dissociation constants agree with some reported in the literature. The application of the model also allows explaining the observed relationship between the apparent formal redox potential and the electrolyte *pH*.

© 2013 Elsevier B.V. All rights reserved.

1. Introduction

Electrochemically active macromolecules (EAM) are substances that can be oxidized and reduced in a reversible way. These macromolecules, both natural and synthetic, have received a great deal of attention. The interest in natural EAM, mostly metalloproteins, is due to its obvious importance in biochemical reactions [1]. On the other hand, the interest in synthetic EAM, mostly in polymers, is due to its potential applications in several fields [2–5].

These macromolecules can be characterized by several properties such as their redox potential, the state of binding, the state of tension (deformation) and the extension of their screening. The redox potential is related to the possibility of the macromolecule to transfer electrons to a suitable redox couple in the same solution or to an electrode submitted to a suitable potential. The state of binding refers to the amount of bound species (mainly ions) on different sites of the macromolecule. The screening refers to the weakening of the electrostatics interactions between the fixed charged sites of the macromolecule due to the ionic atmosphere surrounding them. In this context, the state of tension refers to

conformational deformation that appears in the macromolecule as a consequence of interactions between parts of it.

In a previous work [6], it was shown that a variety of experimental results on EAM can be explained by the existence of couplings among the state of tension, the state of binding, the extension of screening and the redox potential. That is, if one of these states changes, all the others will change too. The vast majority of EAM are polyelectrolytes, and there are many examples of couplings of these types that can be attributed to its polyelectrolytic nature. It is well known that polyelectrolytic macromolecules show couplings among the degree of binding, generally of protons, and its state of deformation [7–9] and screening [10–12]. Deformation can be also induced by redox potential changes [13,14], and changes in the ionic strength of the electrolyte (screening effects) can modify the redox potential in both, natural [15] and synthetic macromolecular systems [16]. Finally, the concept of coupling between the redox potential and proton binding widely spread [17–19]. This coupling is of paramount importance to understand the redox behaviour of proteins, substances in which their redox activity may depend on small changes of the binding ion activity [19–22].

Polyaniline (Pani) is a relatively simple synthetic polymer, as compared with natural EAM, and its electrochemical behaviour is relatively well understood. The aim of this work is to rationalize,

* Corresponding author.

E-mail address: dposadas@inifta.unlp.edu.ar (D. Posadas).

employing a simple modified a statistical mechanics model, the effect, experimentally observed, of proton binding on the redox potential of Pani.

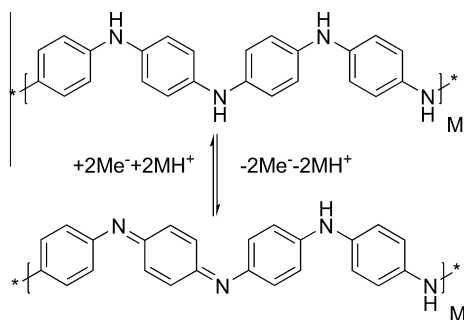
Although simpler than many natural EAM, Pani presents an additional difficulty for the model: its redox potential depends directly on the proton activity in the solution, because protons participate in the redox reaction (Scheme 1). And, as protons also participate in a binding equilibrium with the macromolecule, the redox potential should indirectly depend on the solution *pH* through the coupling effects mentioned above.

In the present work, the coupling between proton binding and the redox potential of Pani, as a particular case of EAM, is experimental and theoretically studied. The experimental investigation of this coupling requires the determination of the oxidation degree of the polymer film in electrolytes of different *pH*s. Contrary to many electrochemical systems, for conducting polymers as Pani, the oxidation degree cannot be simply obtained from the voltammetric or chronoamperometric results because there is a capacitive contribution to the electrochemical current response [23,24]. So, in this work, the oxidation degree is obtained by UV–Visible spectroelectrochemical measurements.

On the other hand, a simple statistical mechanic model is developed to link the redox potential with the oxidation degree and the solution *pH*. The model allows the analysis of the experimental results to determine the proton binding constants of the reduced and the oxidized forms of the polymer, and also other parameters, such as differences in the interaction energy between the redox centres, as a function of the electrolyte *pH*.

2. Materials and methods

Pani films were electro synthesized onto Indium Tin Oxide (ITO) plates ($R_s = 5\text{--}15 \Omega \text{ cm}$, Delta Technologies). These plates were glued to a metallic contact with epoxy silver resin. The top and sides of the metallic plate were covered with an insulating varnish as shown in Fig. 1. The active area of the polymer film onto the ITO plate was around 1.0 cm^2 . The electro synthesis was carried out by cycling the potential at 0.1 V s^{-1} between -0.200 V vs. a saturated calomel electrode (SCE) and a positive potential limit set at the beginning of the monomer oxidation (around $0.700\text{--}0.800 \text{ V}$). To improve the adherence and homogeneity of the film, the positive potential limit was slightly decreased after a few cycles. After the synthesis, the film was washed with pure water and cycled in $3.7 \text{ M H}_2\text{SO}_4$ solution during some minutes and then introduced in the spectrophotometric cell. This was a square quartz cell (Spectrocell, 1 cm side) in which the electrode was inserted perpendicular to the light path. Inside the cell it was placed a Pt plate that serves as the counter electrode, and a fine capillary connected to an external reference electrode (see Fig. 1). This was also a SCE, which was



Scheme 1. Redox commutation for the first redox couple of Pani (only the base forms are shown).

employed throughout the work; all potentials in the text are referred to it. The absorbance of the film electrodes was monitored over a period of several hours and no change was noticed, meaning the Pani film covering ITO plates was stable during that time.

Solutions were made of Milli-Q purified water and NaOH and H_2SO_4 (Carlo Erba, RPE-ACS). The latter were employed as received. A potentiostat TEQ-03 was employed for all the electrochemical experiments.

Spectra were taken with an Agilent model 8453E diode array spectrophotometer in the spectral range comprised between 300 nm and 900 nm and in the potential range between -0.200 and 0.450 V .

Electrolytic solutions of different *pH* and constant ionic strength of 3.7 M of $\text{H}_2\text{SO}_4 + \text{HNaSO}_4$, were employed. For $pH > 1$, the *pH* was measured with a glass electrode adequate for acid media (Ross, Orion Research) by using a *pH*-meter (Cole-Palmer 59003-15). For $pH \leq 1$, the *pH* was measured using a Pd(Pd) hydrogen electrode [25].

Before starting the experiments with each one of the solutions of different *pH* values, the Pani – covered electrodes were polarized at -0.200 V during 20 min to completely reduce and age the Pani films [26,27]. Afterwards, the potential was increased in steps of $0.010\text{--}0.025 \text{ V}$ and held at that potential value for 5 min , to reach ionic equilibrium with the electrolytic solution. Then the spectrum was taken.

As a measure of the film thickness, it was employed the integrated charge from $E = -0.200 \text{ V}$ up to 0.450 V , $Q_T(0.45)$ [24]. Experiments were done with films of charge about $Q_T(0.450) = 32 \text{ mC cm}^{-2}$.

3. Results

In Fig. 2 it is shown the voltammetric response of a typical Pani film between the potential limits -0.200 V and 0.450 V . During the positive half potential scan the reduced form of Pani (Leucoemeraldine, L) is oxidized to the half oxidized form (Emeraldine, E).

The spectra of Pani for different applied potentials, at $pH = -0.60$, are shown in Fig. 3. These spectra show three main characteristic bands in the wavelength range $300\text{--}900 \text{ nm}$. The band at 320 nm is attributed to the $\pi \rightarrow \pi^*$ transitions characteristic of the benzenoid ring units in the polymer. Also, it might be attributed to the band gap in the reduced polymer. This band is the main one for the L form; besides a second broad and small band is observed at about 850 nm . As the polymer is oxidized, the band at 320 nm steadily decreases, a band starts growing at about 400 nm , and the band with a maximum at around 850 nm in the reduced state, shows a gradual increase and shift to 750 nm . These bands are attributed to the polarons and bipolarons associated to the formation of the quinoid units due to the oxidation of the amine to imine groups. Further discussions about the band assignments in Pani spectra are available in several works [28–31].

As the band at 320 nm steadily decreases as the polymer is oxidized; the absorbance changes in this region may be employed to quantify the fraction of oxidized polymer. The relative absorbance change will be defined as:

$$\Delta A(E)_R = \frac{A(E) - A_{0.45}}{\Delta A_T} \quad (1)$$

where $A(E)$ is the absorbance at the potential E , $\Delta A_T = A_{-0.2} - A_{0.45}$ is the total absorbance change and $A_{-0.2}$ and $A_{0.45}$ are the absorbances at $E = -0.2 \text{ V}$ and 0.45 V .

Consequently, the degree of oxidation of the polymer, θ_n , can be expressed as:

$$\theta_n = 1 - \Delta A(E)_R \quad (2)$$

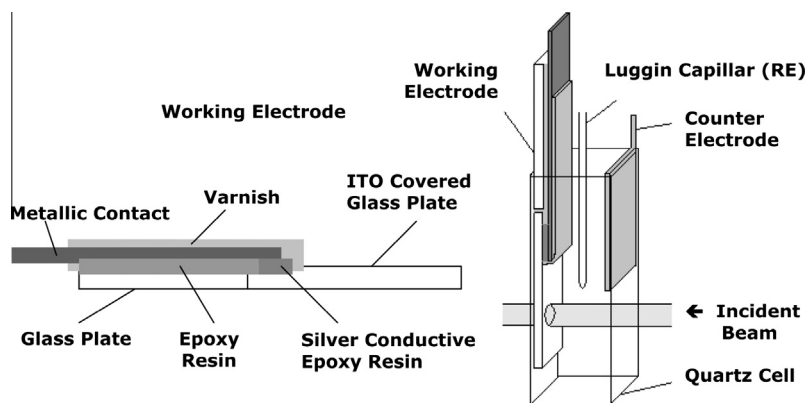


Fig. 1. Schematic representation of the ITO electrode and the cell arrangement.

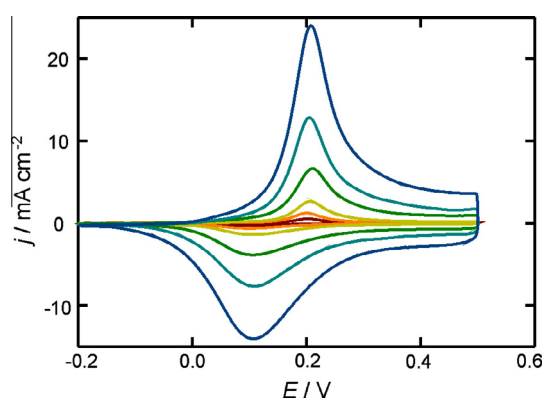


Fig. 2. Voltammetric current potential relationships for a Pani film at different sweep rates, $v/V s^{-1}$: 0.002, 0.005, 0.01, 0.025, 0.05, and 0.1. Electrolyte: 3.7M H_2SO_4 . $Q_T(0.45) = 32.0 mC cm^{-2}$.

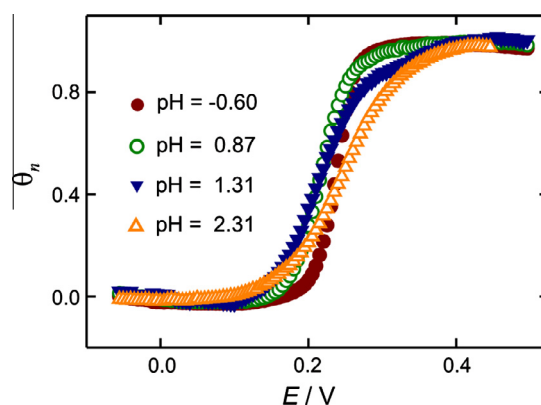


Fig. 4. Oxidation degree as a function of the applied potential for different pH s. $Q_T(0.45) = 32 mC cm^{-2}$.

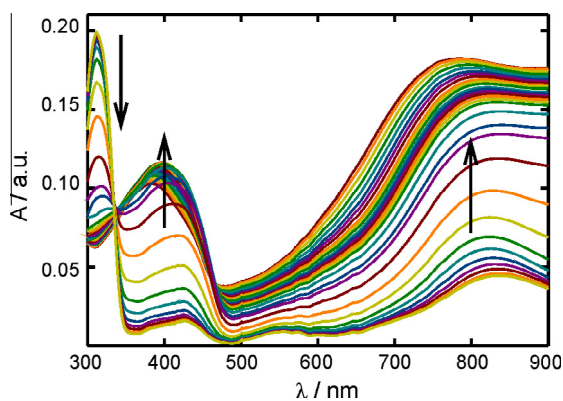


Fig. 3. Pani spectra at different potentials comprised between -0.2 and $0.45 V$ in 3.7M H_2SO_4 ($pH = -0.60$). The arrows indicate the direction of increasing potentials. $Q_T(0.45) = 32 mC cm^{-2}$.

As it can be seen in Fig. 4, the relationship between θ_n and E depends on the solution pH .

4. Theoretical background

4.1. A simple model to show the coupling between the redox potential and the proton binding

The purpose of this section is to present a simple molecular model that shows the coupling between proton binding and the

redox potential for the redox reaction represented in Scheme 1 [32–35]. This model allows a simple statistical thermodynamic analysis of the different contributions that appear in the redox potential of the system, in terms of microscopic quantities, and predicts the form in which these contributions should depend on the external variables.

The simple model employed in the present work is similar to others previously employed [6,36]. A more elaborated model, based on Flory's polymer theory has also been employed [37]. Despite in that model, interactions between polymer segments, between solvent molecules, and between polymer segments and solvent molecules, are explicitly included; it has several disadvantages: First, it is more involved. Second, it needs data about the swelling of the polymer and also other ones such as the "mixture parameter" [37], referred to the polymer that, in general, are not available for EAM.

For brevity this redox reaction will be written as:



where ν_e and ν_H are the stoichiometric coefficients of electrons and protons, respectively.

The redox potential can be obtained from the derivative [38]:

$$E = \frac{RT}{\nu_e F} \left(\frac{\partial A}{\partial n_e} \right)_{T,M,N} \quad (4)$$

where $A = \sum_i \mu_i n_i$ is the chemical part of the Helmholtz free energy of the system, n_i is the number of moles and μ_i refers to all contributions to the chemical potential, except the electrical ones. n_e refers to the number of electrons participating in the reaction (3).

T has the usual meaning of temperature and the quantities M and N will be defined below.

The polymer will be considered as a phase in contact, on one side, with the external solution and, on the other, with a metallic conductor capable of providing holes or electrons for the polymer to be oxidized or reduced, respectively. This phase can be depicted as a polyelectrolyte gel phase composed by intertwined polymer chains, solvent molecules and different ionic species (H^+ , Na^+ , and HSO_4^-) [35–37]. These chains are composed by segments; each one of them is the polymeric unit, as shown in Scheme 1. In the case of Pani, each segment is formed by four monomer units and it is considered that the polymer chains contain a total of M segments. According to the oxidation degree of the polymer, each segment may be oxidized (in number M_{Ox}) or reduced (in number M_R), being $M = M_R + M_{Ox}$. Furthermore, as it is shown in the Scheme 1, each segment has δ redox centres that can be reversibly oxidized or reduced; n_{Ox} and n_R are the number of oxidized and reduced redox centres, respectively. In the case of Pani $\delta = 2$ (see Scheme 1). The total number of centres, $n = n_{Ox} + n_R$, is constant. Moreover, $\delta M = n$, and the fraction of oxidized centres will be defined as $\theta_n = n_{Ox}/n$. Then, according to the stoichiometry of the reaction (3), the differential change in the number of oxidized redox centres will be written as:

$$dn_{Ox} = \frac{dn_e}{v_e} = \frac{dn_H}{v_H} = -dn_R = d\xi \quad (5)$$

where ξ is the degree of advancement of reaction (3). On the other hand, in this description of the system, it is considered that each monomer unit contains functional chemical groups capable of binding protons. In the case of Pani, these are the amine ($-NH-$) and the imine ($-N=$) groups. Depending on the proton activity of the external medium, these groups could be protonated to certain extent, giving rise to charges along the polymer chains ($-NH_2^+$) for the amine groups, and ($-NH^+$) for the imine ones. Let be the number of H^+ , N_R and N_{Ox} , bound to the M_R and M_{Ox} segments, respectively, and the total number of bound protons $N = N_R + N_{Ox}$. Each segment may bind χ protons, and B is the total number of binding sites, then $B = \chi M$. In the case of Pani, the maximum value of χ should be 4. The corresponding coverage degree of protons at the binding sites of M_R and M_{Ox} segments will be defined as $\theta_{N,R} = N_R/\chi M_R$, and $\theta_{N,Ox} = N_{Ox}/\chi M_{Ox}$, respectively.

As the polymer is progressively oxidized some M_R units become M_{Ox} units. After some number of units has been oxidized the polymer will partially become another chemical entity. For instance, in the case of Pani, after two out of four amine units have been oxidized, the reduced unit becomes a half oxidized one.

That is, as the oxidation progress the number of segments of the L form decreases and the number of segments of the E form increases, and M and n remain constant. On the basis of the previous considerations it is clear that $dM_{Ox} = \delta dn_{Ox}$.

For a polyelectrolyte gel the Helmholtz free energy can be written as the sum of four contributions [36,37]: (i) The free energy of mixing the polymer with the solvent, ΔA_m . (ii) The deformation (swelling equilibrium) free energy change, ΔA_d . (iii) The binding free energy change, ΔA_b . (iv) The electrostatic free energy, ΔA_{el} . Explicit expressions for these energies were derived in a previous publication [37]. The derivative of ΔA_b with respect of N_{Ox} defines $\mu_{N,Ox}$, the chemical potential of the proton bound sites on the oxidized segments, and similarly for the proton bound sites on the reduced segments. The derivatives of $\Delta A_m + \Delta A_d$ with respect of M_{Ox} define the chemical potential of the oxidized polymer, $\mu_{p,Ox}$ and similarly for the reduced polymer, $\mu_{p,R}$ [37]. Thus, the terms $\mu_{p,Ox}$ and $\mu_{p,R}$ contain the contributions of mixing and deformation (mechanical effects). It has been shown that the terms $\mu_{p,Ox}$ and $\mu_{p,R}$ are independent of M_{Ox} and M_R , respectively (see comments after Eqs. (13) and (22) in Ref. [37]). This shows, under the assumptions of the model, that $\mu_{p,Ox}$ and $\mu_{p,R}$ do not change during the re-

dox commutation. Therefore, they contribute with a constant amount to the redox potential and this contribution will be included in the standard redox potential. Then, for simplicity, the contributions of deformation and mixing will not be explicitly considered in what follows.

4.2. Thermodynamic considerations

In order to obtain the redox potential is necessary to consider the change in the electrochemical Helmholtz free energy of the reaction (3), \bar{A} . In what follows it will not be explicitly considered mechanical effects (see Ref. [6] and references therein). The change in \bar{A} can be written, at constant temperature, volume, and M , as (see Eq. (15) in Ref. [6]):

$$d\bar{A} = [(\bar{\mu}_{Ox} - \bar{\mu}_R + v_e \bar{\mu}_e + v_H \bar{\mu}_H)] dn_{Ox} + \mu_{N,R} dN + (\mu_{p,Ox} - \mu_{p,R}) dM_{Ox} \quad (6)$$

where $\bar{\mu}_{Ox}$, $\bar{\mu}_R$, $\bar{\mu}_e$ and $\bar{\mu}_H$ are the electrochemical potential of oxidized and reduced redox centres, electrons and protons, respectively. $\mu_{N,R}$ and $\mu_{p,Ox}$ and $\mu_{p,R}$ were defined in the previous paragraph.

The Nernst equation is found by equating to zero the derivative of \bar{A} with respect to the degree of advancement of the reaction (3) [37]. From Eqs. (6) and (4), and considering $dM_{Ox} = \delta dn_{Ox}$, it is obtained [38]:

$$FE = \frac{(\mu_{Ox} - \mu_R)}{v_e} + \mu_e + \frac{v_H \mu_H}{v_e} + \delta \frac{(\mu_{p,Ox} - \mu_{p,R})}{v_e} \quad (7)$$

where $E = \varphi_m - \varphi_{pol}$ is the Galvani potential difference between the metal and the polymer. As μ_{Ox} , μ_R and μ_H should be of the form: $\mu_{Ox} = \mu_{Ox}^0 + kT \ln a_{Ox}$, $\mu_R = \mu_R^0 + kT \ln a_R$, $\mu_H = RT \ln a_H$ and μ_e is constant, it is got:

$$E = E^0 - \frac{RT}{v_e F} \ln \left(\frac{a_R}{a_{Ox}} \frac{1}{(a_H)^{v_H}} \right) = E^0 + \frac{v_H RT}{v_e F} \ln(a_H) - \frac{RT}{v_e F} \ln \left(\frac{a_R}{a_{Ox}} \right) \quad (8)$$

where a_j is the activity of the j species, v_i are the corresponding stoichiometric coefficients, and E^0 is the standard electrode potential. At this point, it must be emphasized that for the case of EAM, E^0 includes the contributions of mixing, deformation (mechanical effects), binding and screening free energies for both, oxidized and reduced, forms of the polymer. Therefore, it is expected E^0 to depend on the pH of the external solution through the proton binding contribution.

The activity ratio, $\frac{a_R}{a_{Ox}}$, can be expressed in terms of the oxidized and reduced fractions and the activity coefficients, γ_i , as:

$$\frac{a_R}{a_{Ox}} = \frac{\theta_R \gamma_R}{\theta_{Ox} \gamma_{Ox}} \quad (9)$$

Being $\theta_{Ox} = \theta_n$, the fraction of the oxidized redox centres, and $\theta_R = 1 - \theta_n$ the fraction of reduced redox centres, E results:

$$E = E^0 - 2.303 \frac{v_H RT}{v_e F} pH - \frac{RT}{v_e F} \ln \left(\frac{\gamma_R}{\gamma_{Ox}} \right) - \frac{RT}{v_e F} \ln \left(\frac{1 - \theta_n}{\theta_n} \right) \quad (10)$$

From Eq. (10), the formal apparent potential, E_{app} , can be defined as the part of the potential that does not explicitly depend on the concentrations of the R and Ox substances. It is important to remark that E_{app} is a magnitude experimentally accessible from the knowledge of the oxidation degree as a function of the applied potential, and does not depend on any model under consideration

$$E_{app} = E + \frac{RT}{v_e F} \ln \left(\frac{1 - \theta_n}{\theta_n} \right) = E^0 - 2.303 \frac{v_H RT}{v_e F} pH - \frac{RT}{v_e F} \ln \left(\frac{\gamma_R}{\gamma_{Ox}} \right) \quad (11)$$

5. Analysis of the results and discussion

According to Eq. (10) a special case of E_{app} is the value of the potential E at $\theta_n = 0.5$ ($E_{\theta_n=0.5}$). The values of $E(\theta_n=0.5)$, as determined from plots shown in Fig. 4, are shown in Fig. 5, as a function of the electrolyte pH . As it can be seen in the figure, the dependence of E_{app} on pH is more complex than that predicted by the term $2.303 \frac{v_H RT}{v_e F} pH$ of Eq. (11), as it would be if E° and γ_R/γ_{Ox} were independent of pH . Therefore, it should be concluded that either E° or γ_R/γ_{Ox} , or both, must also depend on the electrolyte pH . This dependence comes from the coupling between the redox potential and the proton binding, mentioned at the Introduction section.

In Fig. 6, E_{app} is represented as a function of θ_n for some pH values. This figure indicates that there is an apparent redox potential distribution. If there was not a redox potential distribution, the plot presented in Fig. 6 would be a straight line parallel to the θ_n axis. Eq. (11) shows that the observed behaviour implies that the ratio of the activity coefficients, γ_R/γ_{Ox} , depends on θ_n . Moreover, it is also observed that the dependence of E_{app} on θ_n is different for each pH value.

In order to explain these experimental facts, a statistical mechanics model was developed focusing in the effect of proton binding. This is the subject of the following section. The corresponding derivations are treated, however, in separated Appendices.

6. Statistical mechanics considerations

The different chemical potentials in Eq. (4) will be obtained from the well known relationship between the Helmholtz free energy and the canonical partition function (PF) of the gel phase as described in Section 4.1.

It will be assumed that the canonical PF of the system, Q , is the product of different contributions considered being statistically independent [6]; so, it is possible to write

$$Q = Q_M Q_n Q_N Q_H \quad (12)$$

where Q_M is the PF of the segments, Q_n is the PF of the redox centres, Q_N is the PF of the bound protons, Q_H is the PF of protons in the internal solution. Expressions for each PF are given in Appendix A.

Then, the potential can be calculated as [6,36]:

$$E = \frac{1}{v_e F} \left(\frac{\partial A}{\partial n_{Ox}} \right)_{T,M,N} = - \frac{RT}{v_e F} \left(\frac{\partial \ln Q}{\partial n_{Ox}} \right)_{T,M,N} \quad (13)$$

Taking into account the interaction between redox centres employing the Bragg–Williams' Approximation [24,36], the following expression for the potential can be derived (see Appendix A).

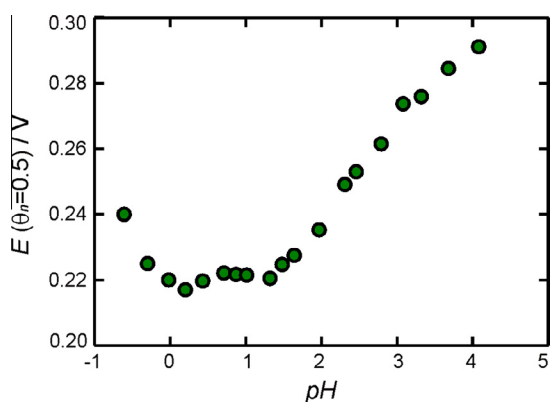


Fig. 5. Dependence of $E_{\theta_n=0.5}$ on the electrolyte pH values.

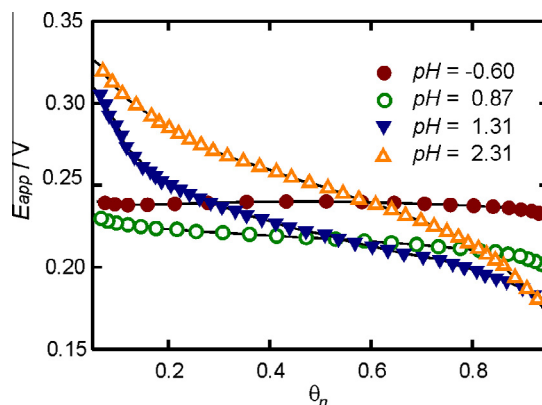


Fig. 6. Dependence of E_{app} on θ_n for data of Fig. 4.

$$E = - \frac{v_H 2.303 RT}{v_e F} pH + \frac{\delta(\mu_{p,Ox} - \mu_{p,R})}{v_e F} - \frac{RT}{v_e F} \times \ln \left(\frac{p_{Ox}^*}{p_R^*} \left(\frac{(1 - \theta_{N,R})}{(1 - \theta_{N,Ox})} \right)^{\chi/\delta} \right) - \frac{\Delta \varepsilon_m}{v_e F} (1 - 2\theta_n) - \frac{RT}{v_e F} \times \ln \left(\frac{(1 - \theta_n)}{\theta_n} \right) \quad (14)$$

The first term on the right hand side (rhs) of Eq. (14) shows the direct effect of the pH on the electrochemical reaction (3). The second term is due to the segments, while the third one accounts for the effect of proton binding (given by the term $\ln [(1 - \theta_{N,R})/(1 - \theta_{N,Ox})]^{\chi/\delta}$). These two terms are implicitly contained in the E° defined above (Eq. (10)). For simplicity, we will refer to these two contributions as E^* . The fourth term contains $\Delta \varepsilon_m$, that is half the energy, per mol, of formation of a pair RR and a pair OO from two pairs OR . This is related to the ratio of the activity coefficients in Eq. (10). Finally, the last term is the usual logarithm of the concentration ratio of the reduced over the oxidized species in the Nernst's equation, Eq. (10). Note that both E^* and $\Delta \varepsilon_m$ should depend on the internal solution pH . Comparing Eq. (14) with Eq. (11), it is possible to derive an expression for E_{app} in terms of the model

$$E_{app} = -2.303 \frac{v_H RT}{v_e F} pH + E^* - \frac{\Delta \varepsilon_m}{v_e F} (1 - 2\theta_n) \quad (15)$$

6.1. The dependence of $\Delta \varepsilon_m$ and E^* on pH

Now, it will be analyzed the dependence of $\Delta \varepsilon_m$ and E^* on pH , in order to obtain the dependence of $\Delta \varepsilon_m$ and E^* on the pH . For this purpose, the interaction between the redox centres will be considered to be coulombic in nature. As the intrinsic charge of the segments is zero, the origin of the fixed charges is the protonation of the centres. As $\theta_{N,Ox}$ and $\theta_{N,R}$ are the mean proton occupancy numbers of the Ox and R sites, under these assumptions, the average charge of one oxidized, z_{Ox} , and reduced, z_R , segment is given by:

$$z_{Ox} = z_{H^+} (\chi/\delta) \theta_{N,Ox} \quad (16)$$

And

$$z_R = z_{H^+} (\chi/\delta) \theta_{N,R} \quad (17)$$

where $z_{H^+} = 1$ is the proton charge. Taking into account the proton binding isotherms (see Appendix B, (Eqs. (B1) and (B2))) and assuming that the interactions between redox centres can be considered as coulombic ones between charged species screened by the ionic atmosphere (see Appendix B), an expression for the $\Delta \varepsilon_m$ dependence on pH can be derived.

$$\Delta\varepsilon_m = C \left[(1 + 10^{pH-pK_{a,ox}})^{-1} - (1 + 10^{pH-pK_{a,R}})^{-1} \right]^2 \quad (18)$$

where C is a constant at constant ionic strength (Eq. (B.10)).

It should be noted here that as a consequence of the fixed charged sites a Donnan potential difference appears at the polymer/solution interface. The maximum concentration of fixed sites has been estimated to be around 2M [29]. With this value in an external solution of 3.7M salt concentration, the Donnan potential can be estimated to be around 10 mV. Then, the difference of proton activity between the external and the internal solution should be very small under these conditions and the pH of the external solution can be used instead of the pH within the film.

Under the same assumptions about the nature of the interaction energy, an expression for the dependence of E^* on pH can be derived. In Appendix B it is shown that:

$$E^* = A_1 + A_2 \left(\left(\frac{1}{1 + 10^{pH-pK_{a,ox}}} \right)^2 - \left(\frac{1}{1 + 10^{pH-pK_{a,R}}} \right)^2 \right) + A_3 \times \ln \left(\frac{1 + 10^{pH-pK_{a,ox}}}{1 + 10^{pH-pK_{a,R}}} \right) \quad (19)$$

where A_1 , A_2 , and A_3 are constants at constant temperature and ionic strength.

7. Analysis of the experimental results in terms of the statistical mechanics model

According to Eq. (15), a plot of E_{app} vs. $(1-2\theta_n)$ should give a straight line of slope $\Delta\varepsilon_m/v_eF$ and ordinate $-2.303 \frac{v_e RT}{v_e F} pH + E^*$ that depends only on pH , as it was explained in reference to Eq. (15). Such plots are shown in Fig. 7 for different pH values. Note also that the ordinates are the values of $E(\theta_n = 0.5)$ at the different pH s. Plots in Fig. 7 are approximately linear in the range $0.3 < \theta_n < 0.7$ and both the slope and the ordinate strongly depend on the pH . This indicates that $\Delta\varepsilon_m$ does change with pH . This behaviour should be expected due to the fact that the charge on the segments must change with the electrolyte pH . On the other hand, the ordinate is expected to depend on the electrolyte pH directly (first term of the rhs of Eq. (15)), and also, indirectly, through the terms $\theta_{N,R}$ and $\theta_{N,ox}$ (see Eqs. 16, 17, B.1, and B.2). The slopes and ordinates of Fig. 7 were obtained by a linear fitting procedure. The resulting values of $\Delta\varepsilon_m$, plotted against the electrolyte pH , are shown in Fig. 8.

In the literature there is agreement that, in the case of Pani, $v_e = v_H = 2$ [32–35], so the ordinate values determined by linear fitting can be used to calculate the term E^* for each pH value. Values of E^* as a function of pH are shown in Fig. 9. From the figure, it can be seen that the contribution of E^* to E_{app} is not negligible.

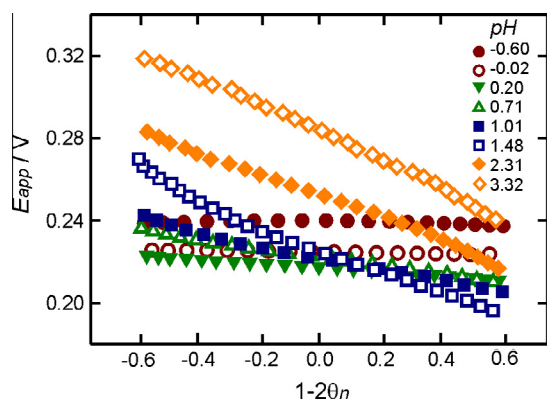


Fig. 7. E_{app} vs. $(1-2\theta_n)$ plot at different pH values.

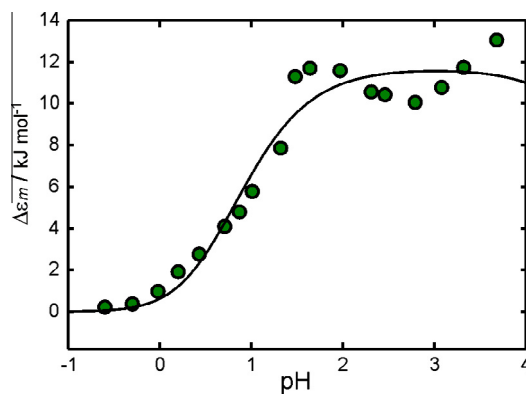


Fig. 8. Dependence of $\Delta\varepsilon_m$ on the pH . The line is the result of the fit to Eq. (18).

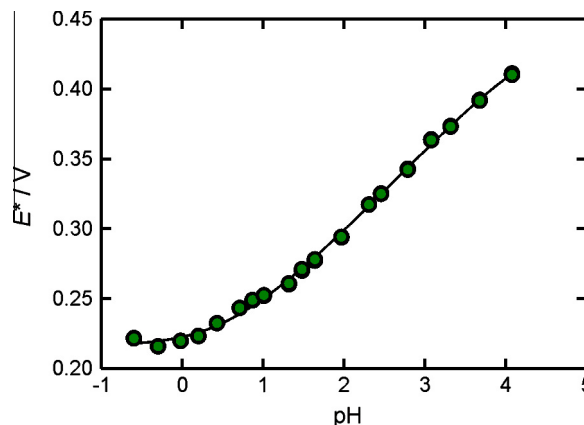


Fig. 9. E^* , calculated from the ordinates of Fig. 7, as a function of pH . The line is the result of the fit to Eq. (19).

Data shown in Fig. 8 can be fitted to Eq. (18). This procedure was carried out with the Levenberg–Marquardt algorithm for non-linear least squares fitting, for the parameters C , $pK_{a,ox}$ and $pK_{a,R}$. The results of the fit are given in Table 1.

Non-linear fitting of the experimental values shown in Fig. 9, to Eq. (19) allows obtaining these constants and the pK_a of each redox form. The resulting values are assembled in Table 2.

From the A_3 value, the relation $\frac{\chi}{\delta}$ can be estimated:

$$\frac{\chi}{\delta} = \frac{-v_e F A_3}{RT} \approx 2 \quad (20)$$

This indicates that the number of binding sites is twice the number of redox centres, in agreement with the reaction shown in Scheme 1 (four binding sites and two redox centres per segment). The values of $pK_{a,ox}$ and $pK_{a,R}$ listed in Table 2 are in reasonable agreement with those reported in Table 1 as well as with those reported in the literature. The value of the oxidized polymer binding constant coincides with that given in the literature [40]. The value of the reduced polymer constant is certainly smaller than the value reported by Menardo et al. [40]. However, it deserves to be mentioned that those authors performed the titration curves on Pani synthesized chemically; experimental procedure that yields the polymer in the shape of a fine grained powder and, therefore, it is difficult to reduce and to reach the protonation equilibrium. On the other hand, *in situ* spectrophotometrical determinations at constant applied potential have allowed us to obtain more reliable values of the pK_a of the reduced form that are about 1 [41]. Comparison with related compounds reinforces this determination [41].

Table 1Results of the fit of data in Fig. 8 to Eq. (18).^a

$B/\text{kJ mol}^{-1}$	$pK_{a,Ox}$	$pK_{a,R}$	r^2
11.8 ± 0.6	5.5 ± 1.5	0.52 ± 0.07	0.987

^a r^2 is the correlation coefficient of the fit.**Table 2**Results of the fitting of the data of E^* and pH according to Eq. (19).^a

A_1/V	A_2/V	A_3/V	$pK_{a,Ox}$	$pK_{a,R}$	r^2
0.2162 ± 0.002	0.015 ± 0.01	-0.0257 ± 0.0006	4.8 ± 0.3	0.9 ± 0.2	0.9998

^a r^2 is the correlation coefficient of the fit.

8. Conclusions

The experimental results for Pani clearly show that there is a formal redox potential distribution and that it depends on pH in a complex way. Not only the mean value (apparent formal redox potential) but also the form of such potential distribution strongly depends on pH . The model presented in this work allows explaining this dependence through the proton binding to the interacting redox centres and then, quantifying the influence of binding on the redox potential. Results could be satisfactorily fitted to obtain several parameters of physicochemical interest, such as the dependence of the interaction energy between the redox centres on the electrolyte pH and the pK_a values of the reduced and oxidized forms.

Acknowledgments

This work was financially supported by the Consejo Nacional de Investigaciones Científicas y Técnicas (PIP 0813), the Agencia Nacional de Promoción Científica Tecnológica (PICT-0407) and the Universidad Nacional de La Plata (UNLP) (Proyecto 11/X590). MIF and DP are members of the CIC of the CONICET. WAM thanks a fellowship of CONICET.

Appendix A

An expression for $(\partial \ln Q / \partial n_{Ox})_{T,M,N,N_{Ox}}$ is needed in order to calculate the potential (Eq. (14)). Then, each component of the PF, Eq. (12), will be analyzed separately.

A.1. The partition function of the segments, Q_M

As discussed in Section 4.1, the contribution of segments to the total free energy is considered to be constant, although different for reduced and oxidized centres, so that

$$(\partial \ln Q_M / \partial n_{Ox})_{T,M,N,N_{Ox}} = -\delta(\mu_{p,Ox} - \mu_{p,R}) / kT \quad (\text{A.1})$$

A.2. The partition function of the redox centres, Q_n

Taking into account the presence of interactions between closest neighbour redox centres, this PF can be written as [24,39]:

$$Q_n(n, n_{Ox}, T) = \frac{n!}{(n - n_{Ox})! n_{Ox}!} (p_{Ox})^{n_{Ox}} (p_R)^{n - n_{Ox}} \left(\exp\left(-\frac{\varepsilon_{OO}}{kT}\right) \right)^{p_{OO}} \times \left(\exp\left(-\frac{\varepsilon_{RR}}{kT}\right) \right)^{p_{RR}} \left(\exp\left(-\frac{\varepsilon_{OR}}{kT}\right) \right)^{p_{OR}} \quad (\text{A.2})$$

where P_{ij} is the number of neighbour pairs $i - j$; p_{Ox} and p_R are the internal PFs of the oxidized and reduced centres, respectively, when no interaction is considered [24]. Here, ε_{RR} , ε_{OO} , and ε_{OR} are the interaction energies between two Ox sites, two R sites and between

one Ox and one R sites, respectively. Within the Bragg–Williams' approximation [39] the number of neighbour pairs, P_{ij} , is calculated as [36]:

$$P_{OO} = \frac{u(n_{Ox})^2}{2n} \quad (\text{A.3})$$

$$P_{RR} = \frac{u(n - n_{Ox})^2}{2n} \quad (\text{A.4})$$

$$P_{OR} = \frac{u(n - n_{Ox})n_{Ox}}{n} \quad (\text{A.5})$$

Being u the number of closest neighbours. So, the expression for Q_n can be written as

$$Q_n(n, n_{Ox}, T) = \frac{n!}{(n - n_{Ox})! n_{Ox}!} (p_{Ox}^*)^{n_{Ox}} (p_R^*)^{n - n_{Ox}} \left(\exp\left(\frac{\Delta \varepsilon_m}{RT}\right) \right)^{n_{Ox}(n - n_{Ox})/n} \quad (\text{A.6})$$

Where the following definitions were employed:

$$\Delta \varepsilon_m = \frac{1}{2} u N_{Av} (\varepsilon_{RR} + \varepsilon_{OO} - 2\varepsilon_{OR}) \quad (\text{A.7})$$

$$p_{Ox}^* = p_{Ox} \exp\left(-\frac{1}{2} \frac{u \varepsilon_{OO}}{kT}\right) \quad (\text{A.8})$$

$$p_R^* = p_R \exp\left(-\frac{1}{2} \frac{u \varepsilon_{RR}}{kT}\right) \quad (\text{A.9})$$

where N_{Av} is Avogadro's number, $\Delta \varepsilon_m$ is half the energy, per mol, of formation of a pair RR and a pair OO from two pairs OR , p_{Ox}^* is the internal PF of an Ox redox centre, p_{Ox} , with its zero energy referred to the energy ε_{OO} , and similarly for p_R^* . Taking into account the preceding expressions, it can be shown that

$$\left(\frac{\partial \ln(Q_n(n, n_{Ox}, T))}{\partial n_{Ox}} \right)_{T,M,N,N_{Ox}} = \ln\left(\frac{(1 - \theta_n) p_{Ox}^*}{\theta_n p_R^*}\right) + (1 - 2\theta_n) \frac{\Delta \varepsilon_m}{RT} \quad (\text{A.10})$$

A.3. The partition function of the binding sites, Q_N

In order to keep the expressions as simple as possible, no interactions between occupied binding sites will be considered. The PF Q_N is the product of PFs of the Ox and R sites. In turn, each one of these is the product of a configurational factor (that is, the ways of distributing N particles among B total free sites) and the contributions of the molecular PF of each occupied site, q . Under these conditions,

$$Q_N(M, M_{Ox}, N, N_{Ox}, T) = \left[\frac{B_{Ox}!}{(B_{Ox} - N_{Ox})! N_{Ox}!} q_{Ox}^{N_{Ox}} \right] \left[\frac{(B - B_{Ox})!}{(B - B_{Ox} - (N - N_{Ox}))! (N - N_{Ox})!} q_R^{N - N_{Ox}} \right] \quad (\text{A.11})$$

where q_{Ox} and q_R are the internal PF of the occupied binding sites in oxidized and reduced segments, respectively, and B is the total number of binding sites ($B = \chi M$), being B_{Ox} and B_R the number of them in oxidized and reduced segments, respectively. Implicitly, it was considered the PF of the empty binding sites to be unity [39]. Employing the Stirling's approximation, the following equation can be derived

$$\left(\frac{\partial \ln(Q_N(M, M_{Ox}, N, N_{Ox}, T))}{\partial n_{Ox}} \right)_{T,M,N,N_{Ox}} = \frac{\chi}{\delta} \ln\left(\frac{(1 - \theta_{N,R})}{(1 - \theta_{N,Ox})}\right) \quad (\text{A.12})$$

Definitions of $\theta_{N,R}$ and $\theta_{N,Ox}$ are given in the main text.

A.4. The partition function of the protons in solution, Q_H

By employing the definitions $(\partial A/\partial n_H)_{T,M,N,N_{Ox}} = \mu_H$, and the stoichiometric restriction given by Eq. (5), $dn_{Ox} = \frac{dn_H}{v_H}$, it is easy to show that:

$$(\partial \ln Q_H/\partial n_{Ox})_{T,M,N,N_{Ox}} = v_H \frac{\mu_H}{RT} = -2.303 v_H pH \quad (A.13)$$

The standard chemical potential of protons in solution is considered to be zero by convention [42].

Employing Eqs. (12), (13), (A.1), (A.10), (A.12), and (A.13), the potential can be then calculated as

$$E = -\frac{v_H 2.303 RT}{v_e F} pH + \frac{\delta(\mu_{p,Ox} - \mu_{p,R})}{v_e F} - \frac{RT}{v_e F} \times \ln \left(\frac{p_{Ox}^*}{p_R^*} \left(\frac{(1 - \theta_{N,R})}{(1 - \theta_{N,Ox})} \right)^{\chi/\delta} \right) - \frac{\Delta \varepsilon_m}{v_e F} (1 - 2\theta_n) - \frac{RT}{v_e F} \times \ln \left(\frac{(1 - \theta_n)}{\theta_n} \right) \quad (A.14)$$

Appendix B

B.1. The isotherm of the proton binding sites

The chemical potential of the bound species on the R sites is found by deriving the logarithm of Q_N with respect to N (see Eq. (6)). Equating this chemical potential to the chemical potential of the protons in solution, the binding isotherm results [39]:

$$\theta_{N,Ox} = \frac{K_{N,Ox} a_{H+}}{(1 + K_{N,Ox} a_{H+})} \quad (B.1)$$

Similarly, for the R sites, it is obtained:

$$\theta_{N,R} = \frac{K_{N,R} a_{H+}}{(1 + K_{N,R} a_{H+})} \quad (B.2)$$

where $K_{N,Ox}$ and $K_{N,R}$ are the proton binding constants for the oxidized and reduced segments. It is important to note that $K_{a,Ox} = 1/K_{N,Ox}$ and $K_{a,R} = 1/K_{N,R}$ are the dissociation constants of the oxidized and reduced centres. Both isotherms are of the Langmuir type and this is a consequence of neglecting interactions between the bound sites.

B.2. The dependence of $\Delta \varepsilon_m$ on pH

The coulombic interaction energy between two spherical charges 1 and 2 of radius a , allowing for screening effects, is [39]:

$$\varepsilon_{12}^{coul}(r > a) = \frac{z_1 z_2 e^2}{4\pi \varepsilon (1 + a\kappa)} \frac{1}{r} \exp(-\kappa(r - a)) \quad (B.3)$$

where z_1 and z_2 are the magnitude of the charges, e is the charge of the electron, r is the distance between the charges, $r_D = 1/\kappa$ is the Debye length and $\kappa^2 = (e^2/\varepsilon kT) \sum_i m_i z_i^2$. $\varepsilon = \varepsilon_0 \varepsilon_r$, is the dielectric constant, being $\varepsilon_0 = 8.8510^{-12} \text{ C}^2 \text{ N}^{-1} \text{ m}^{-2}$ the permittivity in vacuum and ε_r the relative dielectric constant of the medium. The sum is twice the ionic strength and m_i the molality of the i ionic species.

In general, the coulombic interaction between charged species in the presence of ionic screening can be written as $\varepsilon_{12}^{coul} = C'(r, \kappa) z_1 z_2$ where $C'(r, \kappa)$ is a parameter (whose expression is model-dependent) that takes into account the screening effects and of course depends on the ionic strength and the separation between the interacting species. In the case of the redox centres studied here, one can assume that the mean separation between

neighbour centres is constant and, as the ionic total concentration is constant, it follows that

$$\varepsilon_{OO}^{coul} = (z_{Ox})^2 C'(r, \kappa) \quad (B.4)$$

$$\varepsilon_{RR}^{coul} = (z_R)^2 C'(r, \kappa) \quad (B.5)$$

$$\varepsilon_{OR}^{coul} = (z_R z_{Ox}) C'(r, \kappa) \quad (B.6)$$

So that ε

$$\begin{aligned} \Delta \varepsilon_m^{coul} &= \frac{1}{2} u N_{Av} (\varepsilon_{OO}^{coul} + \varepsilon_{RR}^{coul} - 2\varepsilon_{OR}^{coul}) \\ &= (z_{Ox} - z_R)^2 \frac{1}{2} u N_{Av} C'(r, \kappa) \end{aligned} \quad (B.7)$$

By introducing Eqs. (B.1) and (B.2) into the expressions for the segments charges given by Eqs. (16) and (17), and employing the dissociation constants,

$$(z_{Ox} - z_R) = \frac{\chi}{\delta} \left[(1 + 10^{pH - pK_{a,Ox}})^{-1} - (1 + 10^{pH - pK_{a,R}})^{-1} \right] \quad (B.8)$$

being $pK_a = -\log(K_a)$. Then, assuming that $\Delta \varepsilon_m \approx \Delta \varepsilon_m^{coul}$, it results to be

$$\Delta \varepsilon_m = C \left[(1 + 10^{pH - pK_{a,Ox}})^{-1} - (1 + 10^{pH - pK_{a,R}})^{-1} \right]^2 \quad (B.9)$$

where C is:

$$C = \frac{1}{2} \left(\frac{\chi}{\delta} \right)^2 u N_{Av} C'(r, \kappa) \quad (B.10)$$

Note that C is constant at constant ionic strength. Also, note that, in view of Eq. (B.9), for low values of pH , $\Delta \varepsilon_m$ tends to zero (all segments have the same charge and the difference $(z_{Ox} - z_R)$ is zero). Otherwise, this parameter has its maximum value when the highest is the difference of protonation degree of each type of segment.

B.3. The pH dependence of E^* on pH

According to Eqs. (A.7) and (A.8), the quotient p_{Ox}^*/p_R^* includes ε_{OO} and ε_{RR} . The latter depend on the state of charge and so on pH . Taking into account Eqs. (B.4)–(B.6),

$$\begin{aligned} -\frac{RT}{v_e F} \ln \left(\frac{p_{Ox}^*}{p_R^*} \right) &= -\frac{RT}{v_e F} \ln \left(\frac{p_{Ox}}{p_R} \right) \\ &\quad + A_2 \left((1 + 10^{pH - pK_{a,Ox}})^{-2} - (1 + 10^{pH - pK_{a,R}})^{-2} \right) \end{aligned} \quad (B.11)$$

where A_2 is dependent on the ionic strength and the distance between interacting charges. Using this equation and replacing the expressions for the protonation degrees in Eqs. (B.1) and (B.2) in terms of dissociations constants, the potential

$$\begin{aligned} E^* &= \frac{\delta(\mu_{p,Ox} - \mu_{p,R})}{v_e F} - \frac{RT}{v_e F} \ln \left(\frac{p_{Ox}}{p_R} \left(\frac{(1 - \theta_{N,R})}{(1 - \theta_{N,Ox})} \right)^{\chi/\delta} \right) \text{ results to be} \\ E^* &= A_1 + A_2 \left(\left(\frac{1}{1 + 10^{pH - pK_{a,Ox}}} \right)^2 - \left(\frac{1}{1 + 10^{pH - pK_{a,R}}} \right)^2 \right) \\ &\quad + A_3 \ln \left(\frac{1 + 10^{pH - pK_{a,Ox}}}{1 + 10^{pH - pK_{a,R}}} \right) \end{aligned} \quad (B.12)$$

where $A_1 = \frac{\delta(\mu_{p,Ox} - \mu_{p,R})}{v_e F} - \frac{RT}{v_e F} \ln \left(\frac{p_{Ox}}{p_R} \left(\frac{K_{a,R}}{K_{a,Ox}} \right)^{\chi/\delta} \right)$, and $A_3 = -\frac{\chi}{\delta} \frac{RT}{v_e F}$. The first term in Eq. (B.12) is a constant dependent only on the temperature. The second one is related to the dependence of the interaction energies between the redox centres on the pH whereas the third one is related to the dependence of the binding process on the pH .

References

- [1] G. Zubay, *Biochemistry*, fourth ed., Wm. C. Brown, New York, 1998.
- [2] R.W. Murray (Ed.), *Molecular Design of Electrode Surfaces*, Wiley, New York, 1992.
- [3] M.E.G. Lyons, *Electroactive Polymer Electrochemistry*, Plenum, New York, 1996.
- [4] P. Chandrasekar, *Conducting Polymers, Fundamentals and Applications*, Kluwer Academic Publishers, Norwell, MA, 1999.
- [5] Y. Bar-Cohen (Ed.), *Electroactive Polymer (EAP) Actuators as Artificial Muscles: Reality, Potential, and Challenges*, second ed., SPIE, Washington, 2004.
- [6] W.A. Marmisollé, M. Inés Florit, D. Posadas, *Phys. Chem. Chem. Phys.* 12 (2010) 7536–7544.
- [7] C. Tanford, J.G. Buzzell, D.G. Rands, S.A. Swanson, *J. Am. Chem. Soc.* 77 (1955) 6421–6428.
- [8] C. Tanford, *J. Phys. Chem.* 59 (1955) 788–793.
- [9] G. Ybarra, C. Moina, F.V. Molina, M.I. Florit, D. Posadas, *Electrochim. Acta* 50 (2005) 1505–1513.
- [10] J. Mazur, A. Silberberg, A. Katchalsky, *J. Polym. Sci.* 35 (1959) 43–70.
- [11] A. Katchalsky, J. Mazur, P. Spitnik, *J. Polym. Sci.* 23 (1957) 513–532.
- [12] J.G. Voet, J. Coe, J. Epstein, V. Matossian, T. Shipley, *Biochemistry* 20 (1981) 7182–7185.
- [13] L. Lizarraga, E.M. Andrade, F.V. Molina, *Electrochim. Acta* 53 (2007) 538–548.
- [14] L. Lizarraga, E.M. Andrade, F.V. Molina, *J. Electroanal. Chem.* 561 (2004) 127–135.
- [15] J. Petrovič, R.A. Clark, H. Yue, D.H. Waldeck, E.F. Bowden, *Langmuir* 21 (2005) 6308–6316.
- [16] M. Tagliazucchi, F.J. Williams, E.J. Calvo, *J. Phys. Chem. B* 111 (2007) 8105–8113.
- [17] T. Pascher, B.G. Karlsson, M. Nordling, B.G. Malmstrom, T. Vanngard, *Eur. J. Biochem.* 212 (1993) 289–296.
- [18] M. Tagliazucchi, E.J. Calvo, I. Szleifer, *Langmuir* 24 (2008) 2869–2877.
- [19] R. Margalit, A. Schejter, *Eur. J. Biochem.* 499 (1973) 492–499.
- [20] G. Battistuzzi, M. Borsari, D. Dallari, I. Lancellotti, M. Sola, *Eur. J. Biochem.* 241 (1996) 208–214.
- [21] W. Qian, Y.-H. Wang, W.-H. Wang, P. Yao, J.-H. Zhuang, Y. Xie, Z.-X. Huang, *J. Electroanal. Chem.* 535 (2002) 85–96.
- [22] F.A. Leitch, G.R. Moore, G.W. Pettigrew, *Biochemistry* 23 (1984) 1831–1838.
- [23] S.W. Feldberg, *J. Am. Chem. Soc.* 106 (1984) 4671–4674.
- [24] W.A. Marmisollé, M.I. Florit, D. Posadas, *J. Electroanal. Chem.* 655 (2011) 17–22.
- [25] G.J. Hills, D.J.G. Ives, in: D.J.G. Ives, G.J. Janz (Eds.), *Reference Electrodes*, Academic Press, London, 1961.
- [26] W.A. Marmisollé, M.I. Florit, D. Posadas, *J. Electroanal. Chem.* 660 (2011) 26–30.
- [27] W.A. Marmisollé, D. Posadas, M.I. Florit, *J. Phys. Chem. B* 112 (2008) 10800–10805.
- [28] P.M. McManus, S.C. Yang, R.J. Cushman, *J. Chem. Soc. Chem. Commun.* (1985) 1556–1557.
- [29] D.E. Stilwell, S. Park, *J. Electroanal. Chem.* 136 (1989) 427–433.
- [30] D. Chinn, J. DuBow, J. Li, J. Janata, M. Josowicz, *Chem. Mater.* 7 (1995) 1510–1518.
- [31] A.A. Nekrasov, V.F. Ivanov, A.V. Vannikov, *J. Electroanal. Chem.* 482 (2000) 11–17.
- [32] W.S. Huang, A.G. MacDiarmid, *Polymer* 34 (1993) 1833–1845.
- [33] E.M. Genies, M. Lapkowski, C. Tsintavis, *New J. Chem.* 12 (1988) 181–196.
- [34] G. Inzelt, G. Horányi, *Electrochim. Acta* 35 (1990) 27–34.
- [35] M. Kalaji, L. Nyholm, L.M. Peter, *J. Electroanal. Chem.* 313 (1991) 271–289.
- [36] D. Posadas, M. Fonticelli, M.J. Rodríguez Presa, M.I. Florit, *J. Phys. Chem. B* 105 (2001) 2291–2296.
- [37] D. Posadas, M.I. Florit, *J. Phys. Chem. B* 108 (2004) 15470–15476.
- [38] P.D. Atkins, *Physical Chemistry*, sixth ed., Oxford University Press, Oxford, 1998.
- [39] T.L. Hill, *An Introduction to Statistical Thermodynamics*, Addison-Wesley Reading, MA, 1960.
- [40] C. Menardo, F. Genoud, M. Nechtschein, J.T. Travers, P. Hani, in: H. Kuzmany, M. Mehring, S. Roth (Eds.), *Electronic Properties of Conjugated Polymers*, Springer-Verlag, Berlin, 1987.
- [41] W.A. Marmisollé, M.I. Florit, D. Posadas (Unpublished Results).
- [42] K.G. Denbigh, *The Principles of Chemical Equilibrium*, fourth ed., Cambridge University Press, Cambridge, 1981.